Beam Test Results of the BTeV Silicon Pixel Detector

S. Kwan, J.A. Appel, J.N. Butler, G. Cardoso, H. Cheung, G. Chiodini, D.C. Christian, E.E. Gottschalk, B.K. Hall, J. Hoff, P.A. Kasper, R. Kutschke, A. Mekkaoui,R. Yarema, S. Zimmermann
Fermi National Accelerator Laboratory, Batavia, IL 60510, USA
C. Newsom
University of Iowa, Iowa City, IA 52242, USA
A. Colautti, D. Menasce, S. Sala
Sezione INFN di Milano, via Celoria 16 - 20133 Milano, Italy
R. Coluccia, M. Di Corato
Universitá di Milano, Dipartimento di Fisica, via Celoria 16 - 20133 Milano, Italy
M. Artuso and J.C. Wang
Syracuse University, Syracuse, NY 1344-1130, USA

Abstract— **We report the main results of the BTeV silicon pixel detector beam test carried out at Fermilab during the fixed target run 1999-2000. The tests were performed using a 227 GeV/c pion beam incident on a 6 plane silicon microstrip telescope. Several single-chip silicon pixel planes were placed in the middle of the apparatus. The pixel detector spatial resolution has been studied as a function of track inclination and the number of ADC bits. The effect of an applied external magnetic field was also studied.**

Keywords— **BTeV, Pixel, Beam test.**

I. Introduction

Over the last couple of years, Fermilab has gone through two iterations of prototype pixel readout chips (FPIX0 and FPIX1) for the BTeV experiment proposed for the Tevatron [1], [2], [3]. During the 1999 Fermilab fixed target run, tests were performed using both FPIX0 and FPIX1 readout chips bonded to ATLAS prototype pixel sensors. To study the pixel detector spatial resolution, a reference silicon telescope was used to project the incident beam track to the pixel sensor under test. Of particular interest was a comparison of the resolution obtained, using 8 bit and 2 bit charge information, for a variety of incident beam angles (from 0 to 30^0)[4].

In addition, tests were done with a pixel plane in a magnetic field while beam particles traversed the pixel plane and upstream telescopes. In a short test, a diamond target was placed upstream of a four plane pixel telescope, and multi-particle interactions were recorded and analyzed.

II. Experimental setup

The tests were performed in the MTest beamline at Fermilab, with a 227 GeV/c pion beam incident on a 6 plane silicon microstrip telescope (see Figure 1) arranged in two sections, with several single-chip silicon pixel planes placed in the middle of the apparatus. The pixel sensors tested have 50 μm × 400 μm pixel size and are all from the "first ATLAS prototype submission" [5]. Up to four pixel detectors could be tested simultaneously. The silicon microstrip detectors (SSD) were read out using SVX-IIb ASIC's[6] and the data acquisition system was based on VME, adapted from the CDF SVX test stand[7]. The extrapolation accuracy of the silicon microstrip telescope at the pixel detectors location was $\sim$ 2.1 μm for tracks with shared charge in adjacent SSD channels. The excellent spatial resolution was due to the small strip pitch (20 μm) and the high pion momentum available (which minimized the multiple scattering).

The readout was triggered by the coincidence of signals from two 15 cm × 15 cm scintillation counters, positioned upstream and downstream of the silicon telescope and separated from each other by about 10 m. In order to select tracks incident on the active area of the pixel detectors, the FAST_OR output signal from one of the FPIX0-instrumented pixel detectors was also required.

The FPIX0 readout chips were indium bump bonded by Boeing North America Inc. to CiS sensors. The instrumented portion of the sensor is 11 columns × 64 rows. The analog putput from each pixel is digitized by an external 8-bit flash ADC[2].

The FPIX1 readout chips were indium bump bonded by Advanced Interconnect Technology Ltd [8] to Seiko sensors. FPIX1 has 18 columns of 160 rows. However, a minor design error limited the number of rows which may be read out to $\sim$ 90 per column. Each FPIX1 cell contains an amplifier, very similar to the FPIX0 amplifier, and four comparators, which form an internal 2-bit flash ADC[2].

For most of the data taking, the discriminator threshold for the FPIX0 was set to 2500±400 e^- and the amplifier noise was measured to be 105±15 e^-. In addition, we found an equivalent charge noise due to the external buffer amplifier and ADC of 400±150 e^-. The FPIX1 chips have four threshold inputs We found a set of four average threshold values in nominal running conditions, for the FPIX1 of about $3780e^-, 4490e^-, 10290e^-$, and $14680e^-$, with a spread of about $380e^-$. The amplifier noise was measured to be $110 \pm 30e^-$.

III. Results

A. Charge sharing

We have reported in a previous publication results on charge collection, spatial resolution, and resolution function shape[4], [9]. Here we will discuss the resolution as function of cluster size, incident angle, and the number of of ADC bits.

The analog output from the FPIX0 was digitized by a 8-bit FADC. Figure 2 shows the pulse height distribution of a typical pixel for the FPIX0-instrumented detector. The measured pulse height distributions were fit using a Landau function convoluted with a Gaussian [10]. Figure 3 shows the distribution of the most probable signal from all the pixels. This can be fit by a Gaussian with a mean value of 24.3 Ke and a σ of 1025 e^-. Thus, $\Delta Q_{MP}/Q_{MP}$ is measured to be 3.9% and we can conclude that our current calibration procedure limits the usefulness of the analog information to slightly better than 4-bit precision.

The theoretical spatial resolution of a pixel system with $50\mu m$ in the narrow dimension is the pitch ($50\mu m$) divided by $\sqrt{12}$. This value neglects charge sharing and coupling between neighboring pixels. Charge sharing occurs due to charge diffusion, geometry, Lorentz force, and emission of delta rays. Figure 4 shows the cluster sizes as a function of the angle of the incident beam. Even at zero degree(when the beam is normal to the detector), there is charge sharing which could be attributed to diffusion. With increasing angle, the number of single hits (CS=1) decreases and the number of double (CS=2) and treble hits (CS=3) increase, showing the geometrical effects.

B. Spatial Resolution

To study the spatial resolution, beam tracks were fit using data from the SSD telescope and from pixel detectors other than the device under test, using a Kalman-filter. The coordinate measured by a pixel detector is obtained by the position of the center of the cluster of hit pixels associated with a track, plus a correction (conventionally called the η function) which is a function of the charge sharing, the cluster width, and the track angle. For this analysis, we have used a linear "head-tail" algorithm for computing the η function, which ignores the charge deposited in pixels in the interior of a cluster, and uses only the charge deposited on the edges of the cluster[11].

Clearly, the residual distributions are not Gaussian, especially at zero degrees where for a significant fraction of the time only one pixel is hit. The residual distributions also have more entries far from zero than the Gaussian fits. This can be clearly seen in the data taken at ten degrees, when there is always charge sharing. The origin of these "tails" is attributed to the emission of δ-rays which skew the charge sharing and degrade the resolution. Nonetheless, the Gaussian standard deviations provide a reasonably good characterization of the width of the central peak for both plots.

Figure 5 shows the spatial resolution (in the coordinate measured by the 50 μm pixel pitch) for the different cluster sizes using analog readout for an FPIX0-instrumented detector. Figure 6 shows a comparison of the resolution as a function of the incident beam angle achieved by using different number of digitization bits. The plot shows both the resolution obtained using the nominal 8-bit information directly, and also the resolution obtained by degrading the pulse height to 2-bits of information. This result confirms our simulation result that very good resolution can be obtained using charge sharing even with very coarse digitization[12]. Based on these results it has been decided that FPIX2 will have a 3-bit FADC in each pixel cell. This will provide excellent spatial resolution as well as an direct way to monitor any degradation in the performance of the system due to radiation damage. In addition, since the ADC will be implemented using eight independent comparators, some of the thresholds may be used to indicate the presence of delta rays and photon conversions.

We have also computed residual distributions for this data set without using any charge sharing information. These "digital" resolution results are included in Figure 6. Compared to a binary readout, the improvement in resolution even with coarse digitization precision is obvious. The resolution for the FPIX1-instrumented p-stop detector is worse than the results that we obtained by degrading by software the FPIX0-instrumented p-stop pulse height information to 2-bit equivalents. This is because the main effect degrading the resolution is the high threshold and the 2-bit analog information has only a minor effect. In fact, the FPIX1-instrumented detector was operated with a discriminator threshold of ~3780 e^-, while the FPIX0-instrumented detector was operated with a discriminator threshold of ~2500 e^-. To demonstrate this, we have compared the performance between a FPIX0-instrumented detector operated with a threshold of ~3720 e^- and the FPIX1-instrumented detector. The result is shown in Figure 7. There is only a small difference in the spatial resolution and this could be attributed to the effect between 2- and 8-bit analog information. Moreover, the results obtained for a p-spray detector with a threshold of ~2200 e^- show the extent to which the charge losses in the p-spray sensor degrade the spatial resolution.

We have also studied the effect of the applied sensor bias voltage and the discriminator threshold on the spatial resolution. The relative sensitivity of the pixel sensor position resolution to these parameters is very important. In fact, the variation of the bias and effective threshold are similar to what is expected when the radiation damage influences the sensor bulk properties and the charge collection efficiency. The data show, for large track angles, not too much sensitivity to the bias voltage, because the charge-sharing is dominated by the track inclination. At small track angle, when the diffusion gives a substantial contribution to the charge-sharing, the sensor bias is important. The effect of the readout threshold is always significant, but the spatial resolution is still better than $10\mu m$ up to a threshold of $4000e^-$.

C. Multi-particle interactions

Towards the end of the run, we took data with as many as four pixel detectors in a telescope configuration. These four pixel planes were placed between the upstream and downstream sections of the silicon strip detectors. A 2.2mm thick diamond target, was placed upstream of the four-plane pixel telescope. Multiparticle interactions were recorded by triggering on events with pulse height on the downstream scintillation counter consistent with at least three charged particles. Figure 8 shows one of the typical events. Seven tracks were reconstructed using the information from only the four pixel planes. This illustrates the pwer of a pixel telescope in reconstructing events withg high multiplicity. The charge density and hence occupancy per chip observed in these events are much higher than the expected rate that we will get in the BTeV pixel detector system. Also, very few hits that are not associated with the reconstructed tracks are observed in these events even though we did not use the time stamping feature of the readout chips. This demonstrates the low noise characteristics of the pixel system.

D. Magnetic Field

Charge carriers moving in an electric field in the presence of a magnetic field experience the Lorentz force which is perperdicular to the carrier's direction of motion and the magnetic field. This results in a shift of the position at which the carriers arrive at the collecting electrode compared to the case when there is no magnetic field. When the incident beam is normal to the detector, both polarities of the magnetic field have the same effect; i.e. the charge spreads over an increased area. On the other hand, when the incident beam is at an angle to the detector, the polarity of the magnetic field determines whether the charge spread increases or decreases compared to the zero magnetic field case. By comparing the charge spread, we can get a rough estimate of the qualitative effect of the magnetic field.

For this test, a table-top magnet was placed behind the downstream section of the SSD telecsope and a FPIX0-instrumented pixel detector was mounted in the fringe field of the magnet. The pixels were oriented in such a way that the carrier motion in the $50\mu m$ direction was influenced by the Lorentz force. Due to the large force acting on the simple mechanical support for the pixel detector, there was a small tilt between the incident beam and the pixel detector.

Figure 9 shows the fraction of double hits as a function of the magnetic field. The increase in this fraction for larger field strength is clearly visible. Because of the small tilt between the beam and the detector, this fraction shows a minimum at a field strength larger than zero. This happens when the effect due to the geometry cancels out the effect due to the magnetic field. Work in in progress to simulate the setup and to understand better the systematics.

IV. Conclusion

We have described the results of the BTeV silicon pixel detector beam test. The pixel detectors under test used samples of the first two generations of Fermilab pixel readout chips, FPIX0 and FPIX1, (indium bump-bonded to ATLAS sensor prototypes). The spatial resolution achieved using analog charge information is excellent for a large range of track inclination. The resolution is still very good using only 2-bit charge information. The resolution is observed to depend dramatically on the discriminator threshold, and it deteriorates rapidly for threshold above $4000e^-$.

We have also tested a four-plane pixel telescope. Multiple particles have been reconstructed and high multiplicity events could be easily handled. The presence of a magnetic field influences the amount of charge sharing between the pixels which results in a change in the fraction of double hits as the field strength is changed.

References

[1] *BTeV proposal, May 2000*

[2] D.C. Christian, et al., *Nucl. Instr. and Meth.* **A 435** (1999) 144.

[3] C. Newsom, *Overview of the BTeV Pixel Detector*, to be published in the Proceedings of the PIXEL2000 Workshop, Genoa, Italy, June 5-9, 2000.

[4] G. Chiodini, et al., *Beam Test Results of the BTeV Silicon Pixel Detector* , to be published in the Proceedings of the PIXEL2000 Workshop, Genoa, Italy, June 5-9, 2000, FERMILAB-Conf-00/219E.

[5] T. Rohe, et al., *Nucl. Instr. and Meth.* **A409** (1998) 224.

[6] T. Zimmerman, et al., *IEEE Trans. Nucl. Sci.* **Vol.40** No.4 (1993) 736.

[7] S. Zimmerman, et al., *IEEE Trans. Nucl. Sci.* **Vol.43** No.3 (1996) 1170.

[8] S. Cihangir, S. Kwan, *Characterization of Indium and Solder Bump Bonding for Pixel Detectors*, to be published in the Proceedings of the 2nd International Workshop on Radiation Effects in Semiconductor Materials, Florence, Italy, June 25-29, 2000, FERMILAB-Conf-00/168E.

[9] J.C. Wang, et al., *BTeV test beam results*, to be published in the Proceedings of the VERTEX2000 Workshop, Michigan, September 11-15, 2000.

[10] S. Hancock, et al., *Nucl. Instr. and Meth.* **B1:16** (1984) 16.

[11] R. Turchetta, *Nucl. Instr. and Meth.* **A 335** (1993) 44.

[12] M. Artuso, *Spatial resolution predicted for the BTeV pixel sensor*, to be published in the Proceedings of the PIXEL2000 Workshop, Genoa, Italy, June 5-9, 2000.

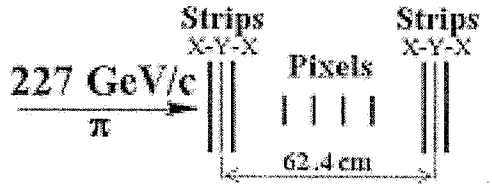

Fig. 1. Schematic drawing of the silicon telescope.

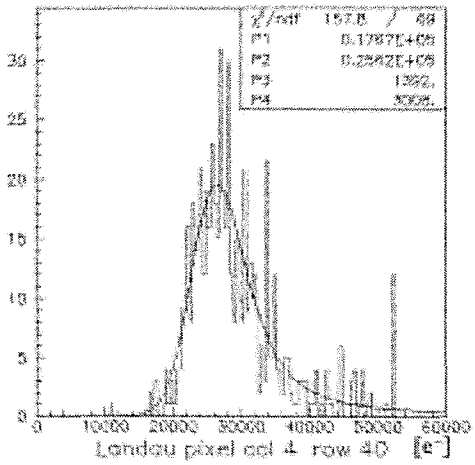

Fig. 2. The typical pulse height distribution observed in a single pixel

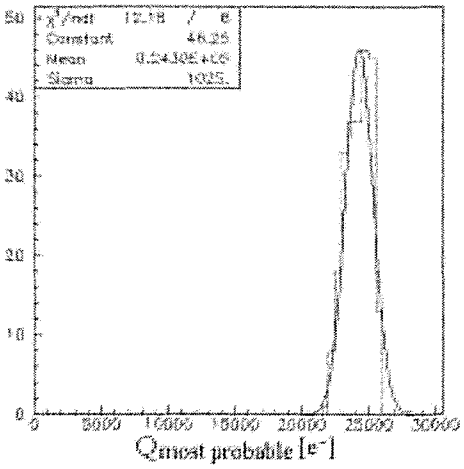

Fig. 3. The distribution of the most probable signal from a beam particle incident on each pixel

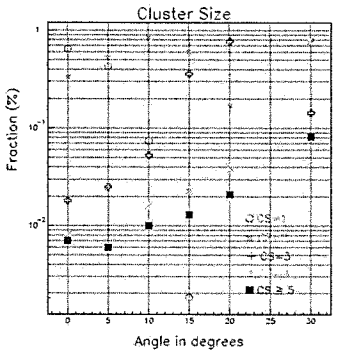

Fig. 4. Cluster size as a function of the incident beam angle

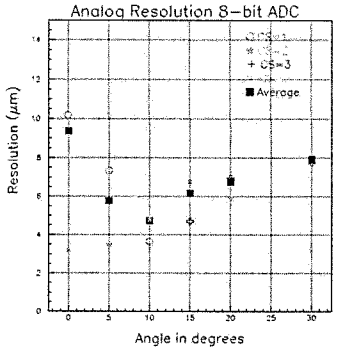

Fig. 5. Spatial resolution for different cluster sizes as a function of the incident beam angle for a FPIX0-instrumented detector

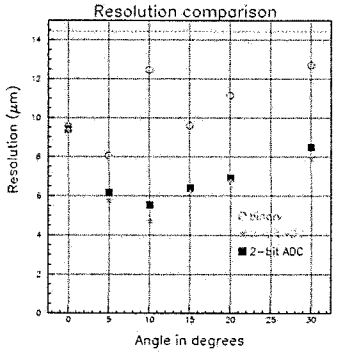

Fig. 6. Resolution for a FPIX0 instrumented detector as a function of incident beam angle using 8-bit, 2-bit analog information and binary readout

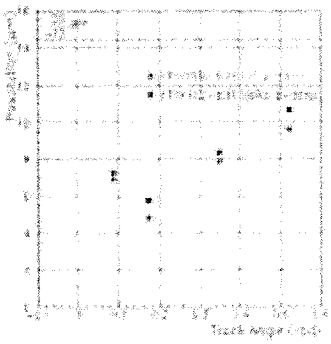

Fig. 7. Comparison of the performances of a FPIX0-instrumented detector and a FPIX1-instrumented detector. The FPIX0 instrumented detector was operated at a threshold of 3720 e^- for this study.

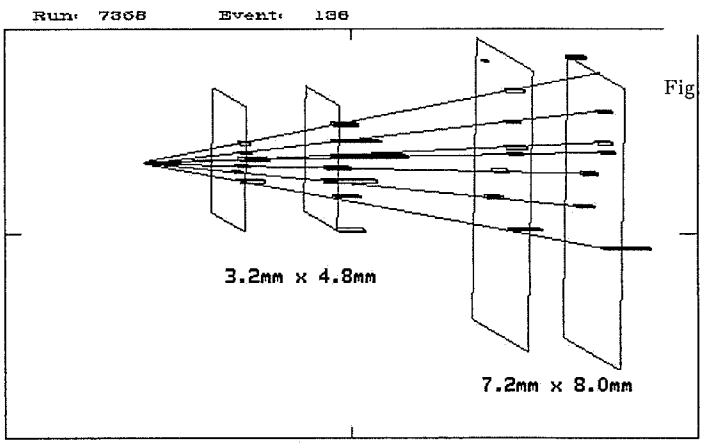

Fig. 8. Multiparticle interaction observed in Fermilab beam test.

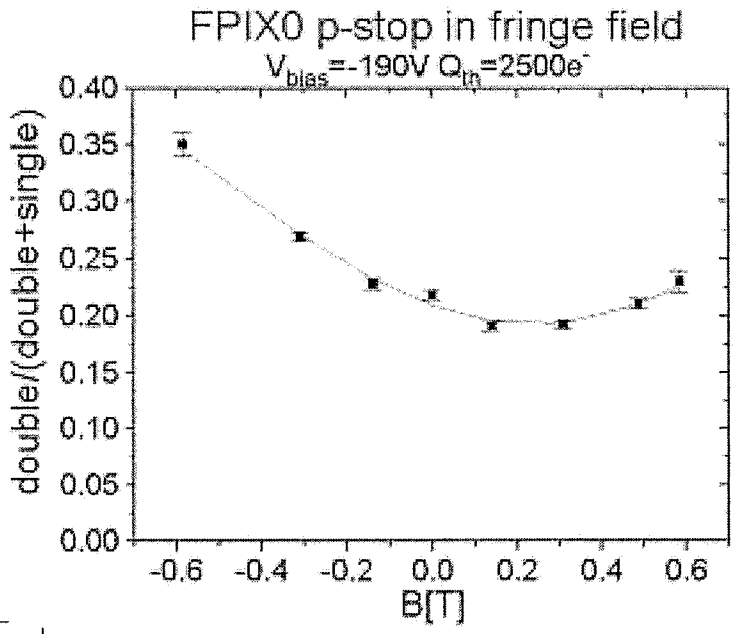

Fig. 9. Ratio of double hits versus the sum of single and double hits as a function of the magnetic field. The curve is a fit to a parabola.